

(Wiley, New York, 1967), pp. 256-259.

<sup>23</sup>R. A. Keller and H. E. Rast, *J. Chem. Phys.* **36**, 2640 (1962).

<sup>24</sup>R. H. Tredgold, *Phys. Soc. Proceedings* **80**, 807 (1962).

PHYSICAL REVIEW B

VOLUME 7, NUMBER 4

15 FEBRUARY 1973

## Energy Transfer between Antimony and Manganese in the Fluorophosphate Phosphors

Thomas F. Soules, Robert L. Bateman, Ralph A. Hewes, and Eric R. Kreidler  
*Lighting Research and Technical Services Operation, General Electric Company, Nela Park,  
Cleveland, Ohio 44112*  
(Received 26 July 1972)

The kinetics of energy transfer from antimony sensitizer to manganese activator in fluorophosphate phosphors has been studied. The transfer mechanism is identified as an exchange interaction by a comparison of the manganese concentration dependence of experimental quantum yield and emission decay curves with theoretical calculations for dipole-dipole, dipole-quadrupole, and exchange mechanisms. The probability per unit time for the energy transfer by exchange is given by  $P = KR^{16}e^{-2R/L} \sin^2\theta \cos^2\varphi$ , where the empirical parameters are  $K = 48.7 \text{ \AA}^{-16} \text{ \mu sec}^{-1}$  and  $L = 0.55 \text{ \AA}$ . The antimony emission decay curve is found to be exponential in the absence of manganese acceptors, with a lifetime of  $7.65 \pm 0.05 \text{ \mu sec}$ . The subsequent manganese emission decay is found to fit the sum of two exponentials with the main component having a lifetime of  $14.3 \pm 0.5 \text{ msec}$  and the minor component (which comprises only about 3% of the total manganese emission) having a lifetime of  $1.9 \pm 0.1 \text{ msec}$ .

### I. INTRODUCTION

There have been numerous experimental studies of resonant energy transfer between impurity ions in inorganic solids.<sup>1-3</sup> Energy transfer, for instance, is important in the operation of many solid-state lasers utilizing rare-earth and transition-metal ions in various host crystals.

Energy transfer also plays a central role in the halophosphate phosphors containing antimony and manganese impurity ions. These phosphors are the most important commercial phosphors. They are extensively used in fluorescent lamps. In the operation of the lamp, ultraviolet radiation from the mercury discharge is absorbed by the antimony impurity centers. Some of the absorbed quanta are reemitted in a band peaking near 480 nm. Energy is also transferred to the manganese impurity ions which emit in the yellow region of the spectrum. The intensity of the manganese emission band is dependent on the acceptor concentration and is adjusted to provide a suitable white light in the lamp. However, while these gross features of the operation of the phosphor have been known for some time,<sup>4</sup> no detailed study of the energy transfer process has been made. Such a study is of interest not only because of its importance in the operation of the halophosphate phosphors but also because it is a prototype for energy transfer between an  $S^2$  sensitizer and a transition-metal activator.

We present an analysis of the kinetics of energy transfer in fluorophosphate phosphors. We have found that the observed energy transfer can only be

plausibly explained by assuming a nonradiative energy transfer using an exchange mechanism of interaction. The characteristics of the energy transfer more closely resemble those involved in the quenching of triplet states in organic phosphors than they do energy transfer which is induced by dipole-dipole or multipolar mechanisms. Triplet-triplet energy transfer has been extensively studied in organic systems<sup>5</sup> since its discovery by Terenin and Ermolev.<sup>6,7</sup> The importance of exchange interactions in energy transfer in inorganic systems has recently been emphasized by Birgeneau *et al.*<sup>8,9</sup>

We found the careful measurement of the decay of the antimony luminescence to be particularly useful in characterizing the mechanism of energy transfer. It enabled us to determine the parameters in the exchange mechanism and to easily distinguish the mechanism of energy transfer from dipole-dipole and multipolar mechanisms. This would have been difficult if we had used the usual method of simply measuring the quantum yield and an average or apparent lifetime.<sup>1,2</sup> Inokuti and Hirayama,<sup>10</sup> who developed a quantitative theory of energy transfer by the exchange mechanism, emphasized the importance of a careful measurement of the decay of the donor luminescence in attaining a full knowledge of energy transfer.

In order to identify the acceptor centers, we also measured the luminescence and decay properties of the emission band peaking near 575 nm in the fluorophosphate phosphors. From electron-spin-resonance studies,<sup>11</sup> it is known that manganese substitutionally replaces calcium ions at the Ca(I) sites

in the fluorophosphate lattice at low concentrations. From combined optical and electron-spin-resonance data, Ryan and Vodoklys<sup>12</sup> concluded that most of the emission in the "yellow-halo" phosphor is due to these manganese impurity centers. The yellow-halo phosphor contains 0.03 mole of manganese per mole calcium in calcium fluorophosphate.

## II. THEORY

### A. Basic Formalism

The calculation of donor luminescence yield and decay time as a function of acceptor concentration was first given by Förster<sup>13</sup> for energy transfer through an interaction between electric dipoles. Inokuti and Hirayama<sup>10</sup> extended their results to the case of energy transfer by an exchange mechanism. A brief summary is presented here in order to better discuss our results for energy transfer in the fluorophosphate phosphors.

Basic assumptions are that energy transfer between donor ions and back transfer from acceptor ions are not important. More general treatments of energy transfer, which include migration of the excitation in the donor system, have been given.<sup>14,15</sup> We discuss energy transfer in the antimony system in the halophosphate phosphors in Sec. IV. Similarly, no energy transfer from manganese to antimony centers is found in the observation of the manganese luminescence decay (see Sec. IV B).

The other assumptions that are usually made concern the nature of the solution of donors and acceptors. Brownian translational motion of the molecules is assumed slow enough that energy transfer occurs to an acceptor at a definite donor-acceptor distance. A continuous random distribution of acceptors is taken. Also it is assumed that molecular rotation is fast compared to energy transfer. In this case, the energy transfer rate can be averaged over molecular orientations. With the exception of the first, these assumptions are applicable to energy transfer in a liquid solution and are not used here.

Consider a system of energy donors and acceptors. Antimony ions are located at Ca(II) sites in the fluorophosphate lattice with an oxygen atom at the nearest-neighbor halide-ion site to provide the mechanism of charge compensation.<sup>16</sup> The acceptors are manganese ions, which also substitute for calcium ions in the lattice. Both optical<sup>11</sup> and electron-spin-resonance data<sup>17</sup> have determined that  $Mn^{2+}$  substitutes for calcium ions with a strong preference for the Ca(I) site in the fluorophosphate host. A small number of antimony ions are initially excited by a short pulse of radiation at time  $t=0$ . Figure 1 shows the arrangement of Ca(I) and Ca(II) sites in calcium fluorophosphate.<sup>18</sup>

In the presence of acceptors the antimony ion

will decay according to

$$n_i^*(t) = n_i^*(0) \exp \left( -\frac{t}{\tau} - \sum_a t P_i(R_a) \right). \quad (1)$$

$n_i^*$  is the probability that the  $i$ th antimony ion is excited.

$1/\tau$  is the intrinsic donor decay rate due to radiation and internal quenching and  $P_i(R_a)$  is the rate of energy transfer from the  $i$ th donor to an acceptor at  $R_a$ . Antimony ions will decay with different decay rates if they have different acceptor environments. The macroscopically significant luminescence decay is proportional to the statistical average of Eq. (1), over antimony ions

$$\Phi(t) = \langle n_i^*(t) \rangle \\ = e^{-t/\tau} \left[ \frac{1}{N} \sum_{a,i} e^{-tP(R_a, \theta_a, \phi_a; \theta_i, \phi_i)} X_a(R_a, \theta_a, \phi_a) \right]^N. \quad (2)$$

Here  $N$  is the number of acceptors in a volume  $V$  and  $X_a(R_a, \theta_a, \phi_a)$  is the probability of finding an acceptor at  $R_a$  with an orientation  $\theta_a, \phi_a$  relative to the crystal axes. The sum over  $i$  sums over orientations of donor ions. In the limit that  $N \rightarrow \infty$ , Eq. (2) can also be written in the form

$$\Phi(t) = e^{-t/\tau} \exp \left( - \sum_{a,i} [1 - e^{-tP(R_a, \theta_a, \phi_a; \theta_i, \phi_i)} \times X_a(R_a, \theta_a, \phi_a)] \right). \quad (3)$$

Equation (2) is perfectly general for pulse excitation.<sup>19</sup> It may be solved numerically if the energy transfer rate to each of the acceptors in a volume  $V$  is known along with the detailed distribution of

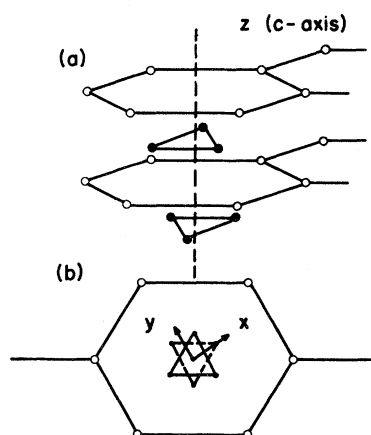


FIG. 1. The Ca(I) and Ca(II) sites in calcium fluorophosphate. The solid circles are Ca(I) sites and the open circles are Ca(II) sites. (a) An oblique angle nearly perpendicular to the  $c$  axis. (b) The  $c$  axis is directed up from the plane of the paper. Not shown are the fluoride ion positions located in the center of the triangles of Ca(II) sites and the arrangement of phosphate groups.

all the ions.

The total donor luminescence yield, which is defined as the ratio of the luminescence yield in the presence of acceptors to that in the absence of acceptors, is given by

$$\frac{I}{I_0} = \frac{1}{\tau} \int_0^\infty \Phi(t) dt. \quad (4)$$

Dexter<sup>20</sup> has derived the following expression for the probability per unit time that energy transfer will occur between two ions:

$$P(R) = (2\pi/\hbar) |\langle \psi_s \psi_a | H_{\text{int}} | \psi_a \psi_s \rangle|^2 \int g_s(E) g_a(E) dE, \quad (5)$$

where  $\psi_s^*(a)$  and  $\psi_s(a)$  are the excited and ground-state wave functions, respectively, of the sensitizer  $s$  and activator  $a$  ions. The integral is over the normalized emission band shape of the sensitizer and absorption band of the activator. The emission band of the antimony ion overlaps the energy levels of several excitation bands of manganese, suggesting that energy-conserving resonance transitions can occur to perhaps more than one excited state of manganese.

#### B. Interaction Mechanisms

We now consider possible interaction mechanisms. In Sec. IV we show that only a short-range exchange interaction is consistent with the donor yield and decay characteristics. Nevertheless, it is useful to obtain order-of-magnitude estimates of the decay rate by using Eq. (5).

The antimony defect states of interest are given in a molecular-orbital calculation by Soules, Davis, and Kreidler.<sup>21</sup> Consideration of their results suggests that excitation of the antimony impurity ion to delocalized  $^1P$  states is followed by rapid relaxation and intersystem crossing to the lowest  $^3P$  states mainly oriented perpendicular to the  $c$  axis of the crystal. This is in agreement with the observed polarization of the emission.<sup>22</sup> The important states of the manganese ( $d$ )<sup>5</sup> configuration are the ground state,  $^6S$  in the weak-field scheme, and the excited states derived from the quartets  $^4G$ ,  $^4P$ ,  $^4D$ , and  $^4F$ . Narita<sup>23</sup> has published a calculation of the crystal field effects of the Ca(I) site on the ( $d$ )<sup>5</sup> configuration of manganese. Their results indicate that the absorption bands at 400 nm are derived mainly from the  $^4G$  atomic levels, the orbital degeneracy being completely removed by the  $C_3$  symmetry of the Ca(I) site.

Hence we write

$$P(\vec{R}) = (2\pi/\hbar) |\langle ^3P(\text{Sb})^6S(\text{Mn}) | H_{\text{int}} | ^4G(\text{Mn})^1S(\text{Sb}) \rangle|^2 \times \int g_s(E) dE. \quad (6)$$

Because the ground and excited states on both the donor and acceptor ions have different spin multi-

plicities, an electronic multipolar interaction will be finite only through the intermediary of spin-orbit coupling on each ion.

Dexter has studied the multipolar expansion of the Coulombic interaction and expressed the matrix elements of  $H_{\text{int}}$  in terms of oscillator strengths, absorption coefficients, and decay times, all of which are measurable quantities. Dexter's expression for the dipole-dipole energy transfer rate is

$$P_{\text{av}}^{\text{dd}}(R) = \frac{3\hbar^4 c^4 Q_a}{4\pi R^6 n^4 \tau} \int \frac{g_s(E) g_a(E)}{E^4} dE. \quad (7)$$

We have assumed the field strength in the medium is equal to that in air.  $Q_a$  is the integrated absorption coefficient for the acceptor ion.  $\tau$  is the intrinsic lifetime of the sensitizer. Other symbols have their usual meaning.

Because the small absorption coefficient of manganese is difficult to measure, we use the modified Einstein relation derived by Fowler and Dexter<sup>24</sup> to obtain the absorption coefficient from our measured value of the emission lifetime 14.3 msec:

$$Q_a = \frac{1}{\tau} \frac{1}{n^2} \frac{h}{4} \left( \frac{g^*}{g} \right) \left( \frac{\lambda_{\text{em}}^3}{\lambda_{\text{abs}}} \right) \text{erg cm}^2 \\ = 1.02 \times 10^{-22} \text{ eV cm}^2. \quad (8)$$

We use  $g^* = 36$  and  $g = 6$ , summing over all the states derived from  $^4G$  and  $^6S$ , respectively.  $n = 1.63$ ,  $\lambda_{\text{em}} \approx 580$  nm, and  $\lambda_{\text{abs}} \approx 510$  nm. Our computed oscillator strength is

$$f = \frac{9n}{(n^2 + 2)^2} \left( \frac{mc}{\pi e^2 \hbar} \right) Q_a \\ = 6.26 \times 10^{-7}.$$

This compares with  $4 \times 10^{-7}$  obtained by Ryan *et al.*,<sup>17</sup> from absorption measurements on single crystals. The agreement between the oscillator strength obtained from absorption measurements and the value calculated using the modified Einstein relation confirms the suggestion by Fowler and Dexter that changes in transition moments between absorption and emission that can cause large discrepancies are probably not as important in  $\text{Mn}^{2+}$  defect centers.

From emission and absorption spectra, we estimate the spectral overlap integral

$$\int \frac{g_s(E) g_a(E)}{E^4} dE \approx 8.2 \times 10^{-3} \text{ eV}^{-5}.$$

Substituting in Eq. (7) gives

$$P^{\text{dd}} = \frac{1}{\tau} \left( \frac{4.02}{R} \right)^6.$$

Hence within the lifetime of the donor excitation only those acceptor ions within a radius of around 4.02 Å will be sensitized. We show in Sec. IV

that a value of  $R_0 = 9.75 \text{ \AA}$  is required to account for the donor yield. This corresponds to an energy transfer rate over two orders of magnitude greater than that predicted for dipole-dipole coupling.

Dexter showed that dipole-dipole interactions can generally be expected to dominate the energy transfer mechanism when both the sensitizer and activator are characterized by allowed dipole transitions. In the case of energy transfer to manganese, the dipole oscillator strength of the manganese ion is very much smaller than the usual allowed ones. Axe and Weller<sup>25</sup> emphasized that in the case of rare-earth ions, for example, where transitions within the  $(f)^n$  configuration are nominally forbidden, the order of dipole-dipole, dipole-quadrupole, and quadrupole-quadrupole interactions can sometimes be expected to be inverted. This is true even though quadrupole radiative transitions cannot favorably compete with dipole processes. As pointed out by Dexter, there is no contradiction in this, since in radiative processes the quadrupole oscillator strength is reduced by the factor  $\sim (a/\lambda)^2$  over the dipole process.

On the other hand, the ratio of the dipole-dipole to dipole-quadrupole energy transfer rates is easily obtained from Dexter's equations as

$$\frac{P^{\text{dd}}}{P^{\text{dq}}} = \frac{8}{27\alpha} \frac{R^2 |\langle \vec{r}_a \rangle|^2}{|\langle \vec{r}_a \cdot \vec{r}_a \rangle|^2}, \quad (9)$$

where  $\alpha = 1.266$  and  $|\langle \vec{r} \cdot \vec{r} \rangle|^2$  is the double dot product of the dyadic. The dipole moment for the manganese ion is estimated from the oscillator strength

$$f = \frac{16\pi m \pi^2 c}{h\lambda} |\langle \vec{r}_a \rangle|^2, \quad |\langle \vec{r}_a \rangle|^2 = 4.9 \times 10^{-7}. \quad (10)$$

The quadrupole moment must be calculated from the wave function. Because there are no other sextets in  $(d)^5$  and because the ground-state  $^6S$  mixes with only the  $^4P$  states through spin-orbit coupling,<sup>26</sup> the matrix element may be written

$$|\langle \vec{r} \cdot \vec{r} \rangle|^2 = |\langle ^4G | \vec{r} \cdot \vec{r} | ^4P \rangle|^2 \frac{5\rho^2}{[E(^4P) - E(^6S)]^2}, \quad (11)$$

with the wave functions obtained for the manganese ion by Clogston,<sup>27</sup>

$$|\langle ^4G | \vec{r} \cdot \vec{r} | ^4P \rangle| \approx \langle r^2 \rangle (\frac{2}{10})^{1/2} \frac{4}{7}.$$

Therefore, using  $\langle r^2 \rangle = 0.46 \text{ \AA}^2$ ,<sup>28</sup>  $\rho = 200 \text{ cm}^{-1}$ ,<sup>29</sup> and  $E(^4P) - E(^6S) = 30500 \text{ cm}^{-1}$  (the mean of Narita's crystal field levels<sup>23</sup>), we deduce

$$P^{\text{dd}} = 3.9 \times 10^{-2} R^2 P^{\text{dq}}.$$

Hence the dipole-quadrupole interaction is computed to be greater than the dipole-dipole transfer

rate out to around  $5 \text{ \AA}$ . At greater distances the dipole-dipole interaction dominates. Using the above estimate for the quadrupole transition moment of manganese gives an energy transfer rate for the dipole-quadrupole interaction mechanism of

$$P^{\text{dq}} = \frac{1}{\tau} \left( \frac{4.20}{R} \right)^8.$$

As we show in Sec. IV, this is more than three orders of magnitude too small to account for the energy transfer. We conclude from this, and similar considerations applied to other terms, that neither electric nor magnetic multipole interactions can account for the observed energy transfer in halophosphate phosphors.

We now consider the exchange interaction  $H_{\text{ex}}$ . The matrix element of the exchange interaction reduces to integrals of the following type when suitable determinantal wave functions are substituted into Eq. (6):

$$\begin{aligned} \langle H_{\text{ex}} \rangle = s \iint \Phi_{5p}^*(r_1) \Phi_{3d_1}^*(r_2) \frac{1}{r_{12}} \Phi_{3d_j}(r_1) \Phi_{5s}(r_2) d\tau_1 d\tau_2 \\ \times \iint \chi_{5p}^*(\sigma_1) \chi_{3d_1}^*(\sigma_2) \chi_{3d_j}(\sigma_1) \chi_{5s}(\sigma_2) d\sigma_1 d\sigma_2, \quad (12) \end{aligned}$$

where  $s$  is a symmetry factor. These integrals are nonzero only when the spin functions  $\chi_{5p} = \chi_{3d_j}$  and  $\chi_{5s} = \chi_{3d_j}$ . However, it is clear that, in general, the exchange interaction will couple the wave functions without invoking the spin-orbit intermediate coupling. The magnitude of the coupling will be comparable to the diagonal exchange matrix element in Eq. (12). For an energy transfer time equal to the donor lifetime, we obtain

$$\langle H_{\text{ex}} \rangle = 0.0299 \text{ cm}^{-1}.$$

This is a reasonable value for an exchange interaction even over fairly large distances because of the diffuse nature of the antimony wave functions.

In order to evaluate the exchange integral in Eq. (12) for different donor-acceptor distances, we use the approximation

$$\begin{aligned} \langle H_{\text{ex}} \rangle \approx s \Phi_{5p}^*(\vec{R}_a) \Phi_{5s}(\vec{R}_a) \\ \times \int \int \Phi_{3d_1}(r_2) (1/r_{12}) \Phi_{3d_j}(r_1) d\tau_1 d\tau_2. \quad (13) \end{aligned}$$

Here we have assumed that the wave function on the donor antimony ion is constant at large distances over the volume of a manganese ion. We approximate the donor-impurity wave functions by hydrogenlike atomic orbitals. At distances greater than an atomic radius we can write

$$\begin{aligned} P(R_a, \theta_a, \phi_a; \theta_i, \phi_i) = K(\theta_a, \phi_a) R_a^{4(n-1)} e^{-2R_a/L} \\ \times \sin^2 \theta_i \cos^2 \phi_i, \quad (14) \end{aligned}$$

where  $n = 5$  (principal quantum number),  $L = 5a_0/$

$(Z_{sp}^* + Z_{ss}^*)$ , and

$$K = (2\pi s^2/\hbar) N_{ss}^2 N_{sp}^2 \left| \int \int \Phi_{3d_i} (1/r_{12}) \Phi_{3d_j} d\tau_1 d\tau_2 \right|^2 \\ \times \int g_s(E) g_a(E) dE.$$

At the donor-acceptor distances of interest ( $\geq 4$  Å), this is a good approximation to both the range and angular dependence of the direct exchange integral. Some compensation for electron delocalization and superexchange is obtained by choosing  $L$  and  $K$  empirically. We note that Eq. (14) gives a somewhat longer-range dependence of the exchange interaction than does a simple exponential approximation. Also the exchange interaction is highly anisotropic. If the donor excited-state wave function is oriented along the  $x$  direction shown in Fig. 1, energy transfer is favored in this direction.

### III. EXPERIMENTAL

#### A. Sample Preparation

The fluorophosphate samples coactivated with antimony and manganese of the general formula  $\text{Ca}_{10-x-y}\text{Sb}_x\text{Mn}_y(\text{PO}_4)_6\text{F}_2$  were prepared from calcium orthophosphate intermediates of the general formula  $\text{Ca}_{9-x-y}\text{Sb}_x\text{Mn}_y(\text{PO}_4)_6$ . The orthophosphates were prepared from appropriate amounts of  $\text{Ca}_2\text{P}_2\text{O}_7$ ,  $\text{CaCO}_3$ ,  $\text{Sb}_2\text{O}_3$ , and  $\text{MnCO}_3$ , which were mixed thoroughly under acetone and loaded into silica boats. A two-step firing process was carried out in a nitrogen atmosphere at 800 and 1100 °C for 15 h at each temperature. The orthophosphates were then mixed under acetone with high-purity  $\text{CaF}_2$ . The coactivated samples were placed in new silica boats and fired in nitrogen at 1100 °C for 2 h. Special care was taken with the samples containing manganese but no antimony to prevent contamination by antimony. They were placed in silica capsules and evacuated at 400 °C for 1 h before sealing and firing. Evacuated capsules were also used to fire coactivated samples in which the antimony was charge compensated by sodium instead of oxygen. In this case,  $\text{NaCO}_3$  was also added to the orthophosphate mix.

#### B. Optical Measurements

Emission spectra of the phosphor samples with varying manganese concentrations were recorded to provide quantum yield data. The spectroradiometer system employed for these measurements has been described previously by Davis *et al.*<sup>30</sup>

Luminescence decay curves were obtained using pulsed excitation sources. The apparatus for the study of the antimony emission decay is shown in Fig. 2. The uv source was a deuterium lamp powered by a TRW nsec light pulser (model 88A) which produced a pulse duration of 15 nsec. The optical system consisted of a 253.7-nm interference filter and a quartz lens to focus the exciting light on the

powder sample plaque, followed by another focusing lens and sharp-cutoff filters to isolate the antimony emission. The emission was detected by a photomultiplier tube and analyzed with a PAR boxcar integrator (model 160) which drove an  $xy$  recorder. An accurate time mark to trigger the scan of the boxcar integrator was obtained from a second photomultiplier tube which viewed the pulsed deuterium lamp directly. Antimony emission decay curves were normally recorded over a time interval of 10  $\mu\text{sec}$  starting at 0.33  $\mu\text{sec}$  after the exciting light pulse. The time resolution was 0.1  $\mu\text{sec}$ .

For recording the longer-lifetime manganese emission decay curves, we used a slower, but more intense, source consisting of a General Radio stroboscopes (type 1531-AB) with a xenon flashtube (E. G. & G. FX-108AU). In this case the triggering signal for the boxcar integrator was obtained from the trigger output of the stroboscopes. The increased intensity of the source permitted the use of Bausch & Lomb high-intensity grating monochromators for selection of the excitation and emission wavelengths when variability and resolution were desired.

#### C. Sample Analysis

The samples were analyzed to determine the activator concentrations. The atomic percents of antimony were obtained by standard wet-chemistry techniques, while the manganese concentrations were determined by atomic absorption spectrophotometry.

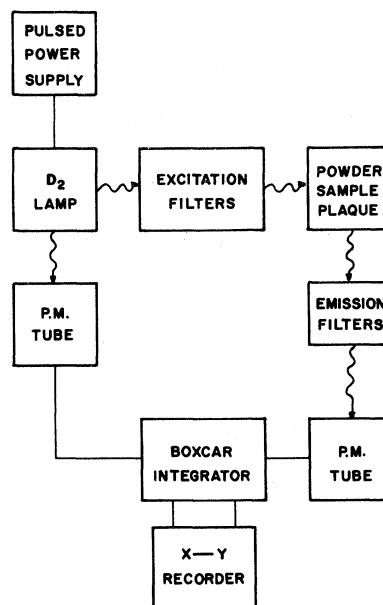


FIG. 2. Diagram of the experimental arrangement used for measuring luminescence decay following pulse excitation.

## IV. EXPERIMENTAL RESULTS AND THEIR ANALYSIS

In this section we present the relative quantum yields of antimony luminescence in a series of phosphors containing antimony and manganese impurities in the fluorophosphate host. We also present the decay curves obtained as described in Sec. III. From an analysis of these results we can determine (1) the precise range dependence of the interaction responsible for energy transfer from antimony to manganese and (2) information on the nature of manganese centers receiving energy from excited antimony defects.

## A. Antimony Luminescence Yield and Decay

It is very useful and reliable to compare theory and experiment with regard to both the donor luminescent yield and decay characteristics for a series of phosphors with different acceptor concentrations. If, for example, the probability per unit time for energy transfer  $P(R_a)$  is the same for all acceptor ions, then it can easily be shown that Eq. (3) gives the donor luminescent decay curve of the form

$$\Phi(t) = e^{-(t/\tau)(1+x/x_0)}, \quad (15)$$

where  $x_0$  is an arbitrary reference concentration. However, this is the only case for which the decay curve is a simple exponential with a decay constant that increases in direct proportion to the acceptor concentration. The yield obtained from Eq. (4) has the so-called Stern-Volmer concentration dependence<sup>31</sup>

$$\frac{I}{I_0} = \frac{1}{1+x/x_0}. \quad (16)$$

In all other cases, where the interaction  $H_{int}$  depends on the distance between the donor and acceptor ions, the donor decay is nonexponential from Eq. (3). At short times [ $t \sum P(R_a) \ll 1$ ] the decay curve approaches

$$\exp\left[-t\left(\frac{1}{\tau} + \sum P(R_a)X_a\right)\right],$$

while at long times ( $tP(R_a) \gg 1$ ) the decay will approach the intrinsic donor decay at a reduced amplitude. If the energy transfer interaction is very short ranged, then the donor decay curve and yield will approach the results obtained for the Perrin model.<sup>32</sup> Perrin proposed that the energy transfer rate is infinite to any acceptor ions within an "active sphere" around the activator and zero outside. This simplified model leads to a decay function of the form

$$Ae^{-t/\tau}. \quad (17)$$

In contrast to the Stern-Volmer model, the decay rate is seen to be independent of the concentration

of acceptors. The intensity of the donor luminescence initially drops to  $A = e^{-x/x_0}$ , at which point the only donors still excited are those with no acceptors within the "active sphere." These decay with the intrinsic decay rate  $\tau$ . The relative yield is given by

$$I/I_0 = e^{-x/x_0}. \quad (18)$$

In Fig. 3, we show the relative quantum yields of antimony luminescence for a series of fluorophosphate phosphors with increasing manganese concentration. Because the antimony and manganese emission bands overlap, the relative quantum yield must be obtained by first determining the emission bands of antimony and manganese in samples containing only one of the ions. A least-squares fit is then made to the spectra of each of the samples containing both ions. The best fit revealed a small shift in the antimony and manganese emission bands which occurred when substantial amounts of the other ion were present. Ryan *et al.*<sup>12</sup> attributed the small shift observed in the manganese emission band in the presence of antimony to a change in the lattice vibrational constants which are responsible for the Stokes shift.

The theoretical yield curve for the exchange mechanism is also shown in Fig. 3. It is obtained by substituting Eq. (14) into Eq. (2) and Eq. (4). In order to obtain convergence to three significant figures, it was necessary to evaluate Eq. (2) for energy transfer to all acceptor-ion sites within 30 Å, which includes 792 Ca(I) sites. The two parameters appearing in Eq. (14) are adjusted to fit one point on the yield versus concentration curve and simultaneously fit the decay curve Fig. 4(b). Once the two parameters are obtained in this way they are used to generate the yield and decay curves for all concentrations. A standard numerical quadrature integration is used for evaluating the integral in Eq. (4). The yield data are in excellent agreement with the theoretical curve over the range of  $Mn^{2+}$  ion concentrations investigated: 0.1–10 at. %.

Figure 3 also shows the results of substituting the forms for the average dipole-dipole and dipole-quadrupole transfer rates, namely,  $(R_0/R)^6$  and  $(R_0/R)^8$ , respectively in Eq. (5). A best fit to the yield data gives  $R_0$  equal to 9.75 and 10.40 Å for the dipole-dipole and dipole-quadrupole interaction mechanisms, respectively. These correspond to energy transfer rates at a given distance from the donor that are, respectively, 200 and 1400 times faster than those computed in Sec. III. Hence they do not represent reasonable values of the dipole and quadrupole transition moments of manganese. They show a yield versus concentration curve that is, however, only slightly flatter than the results of the exchange mechanism. Hence the yield data

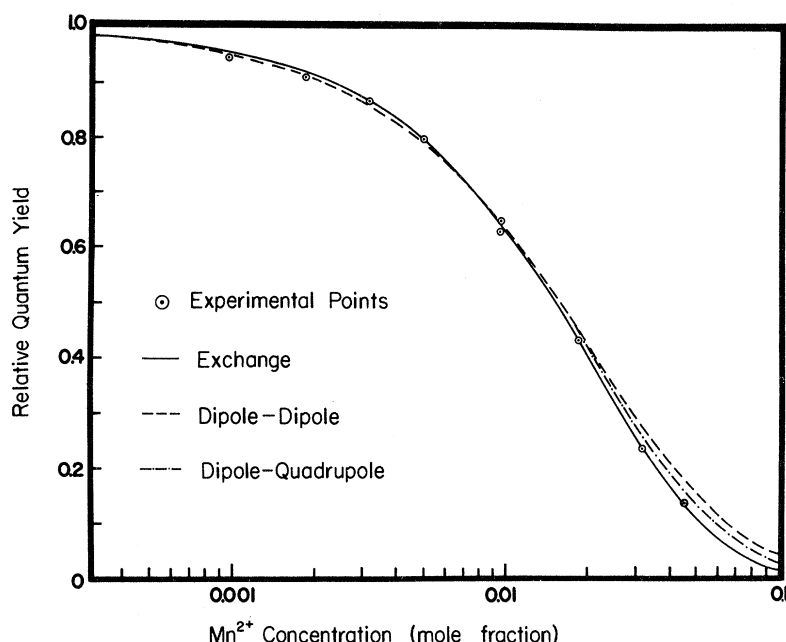


FIG. 3. Antimony luminescence yield versus manganese concentration in fluorophosphate. Circles show the experimental data for the antimony-manganese donor-acceptor concentration series. The theoretical curves are calculated for exchange, dipole-dipole, and dipole-quadrupole energy transfer.

alone are not sufficient to determine the mechanism of energy transfer.

Table I shows the same yield data that are plotted in Fig. 3 and a least-squares fit to the Perrin equation (18). The good fit to the simple Perrin model suggests an exchange interaction that is well defined within a small volume around the donor ions. Similarly the quantum yield of phosphorescence in systems in which triplet-triplet energy transfer occurs is found to fit Eq. (18).<sup>33</sup>

In Fig. 4, we present the antimony emission decay curves in fluorophosphate phosphors. The decay curves were obtained by the method described in Sec. II. The decay of antimony luminescence in phosphors containing no manganese showed an exponential time dependence over several orders of magnitude as expected. The lifetime  $\tau$  is equal to  $7.65 \pm 0.05 \mu\text{sec}$  at room tem-

perature. The error limits given are due to errors in measuring the time base. The fit to an exponential decay was better than one part per thousand for all but long times greater than  $50 \mu\text{sec}$ .

In the presence of manganese ions, the antimony decay curve becomes nonexponential. The nonexponential character of the decay curve is most prominent at short times after the pulse. Hence, the decay curves are shown for the time interval from  $0.33$  to  $10 \mu\text{sec}$ . Further, the early nonexponential drop in the decay curves increases with increasing acceptor concentration of  $0.949$ ,  $1.84$ , and  $4.58$  at. % in Figs. 4(a), 4(b), and 4(c), respectively. However, the drop in the decay curve is much less than that computed for the dipole-dipole and dipole-quadrupole mechanisms. The latter were obtained by substituting  $(R_0^d/R)^6$  and  $(R_0^q/R)^8$  for the energy transfer rate in Eq. (2). The calculations were carried out with the parameters  $R_0^d$  and  $R_0^q$ , which are consistent with the yield data above.

The reason for the apparent discrepancy between the quenching of the donor yield in Fig. 3 and the drop in the decay curve must be due to a large early time decrease in the donor intensity. This qualitative feature discussed before is due to the short-range nature of the exchange interaction and is in agreement with the Perrin model. However, the latter would predict no change in the antimony only decay after time  $t = 0$ . Hence, the observed decrease in the antimony lifetime is a measure of the deviation of the exchange interaction from the well delimited sphere of action of the Perrin model.

TABLE I. Quantum yield of donor luminescence in fluorophosphate phosphors with different manganese concentrations.

Mn <sup>2+</sup> (at. %)	Sb <sup>3+</sup> (at. %)	Sb <sup>3+</sup> Quantum yield	$e^{-x/2.065}$
0.0986	0.33	0.947	0.953
0.186	0.36	0.912	0.914
0.32	< 0.5	0.866	0.857
0.502	0.32	0.797	0.784
0.949	< 0.5	0.628	0.632
0.949	0.25	0.647	0.632
1.843	0.22	0.431	0.410
3.2	< 0.5	0.233	0.212
4.58	0.18	0.103	0.109

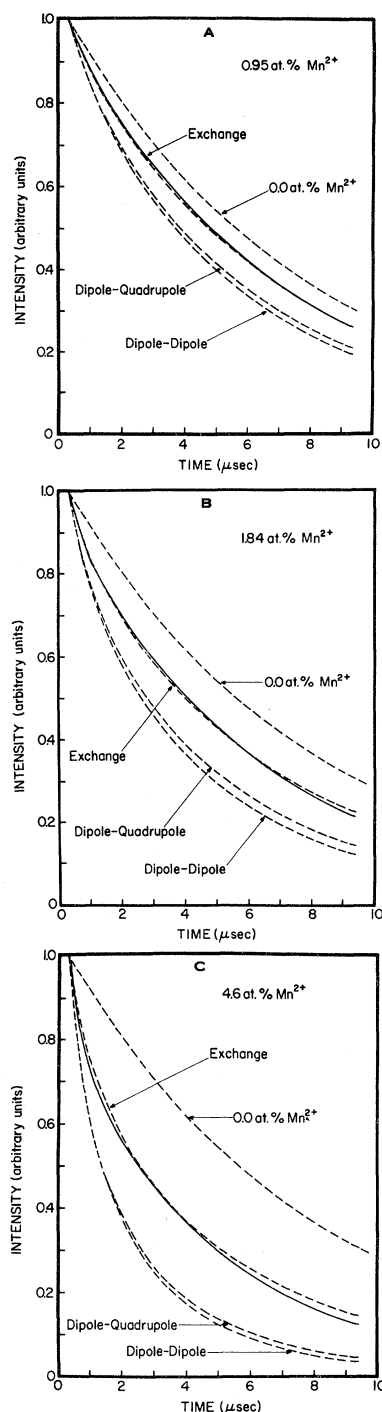


FIG. 4. Decay curves of antimony luminescence in the presence of different manganese concentrations following a light pulse and a comparison with different theoretical models for the energy transfer. The solid curve was made by the integrator which started recording at 0.334  $\mu\text{sec}$  following the light pulse. The lower dashed lines are calculated theoretically for exchange, dipole-quadrupole, and dipole-dipole interactions. The concentration of manganese is given in atomic percent. Also shown is the decay curve of antimony luminescence in the absence of manganese.

TABLE II. Parameters for the exchange interaction.

Quantity	Experimental	Calculated from atomic orbitals
$L$	0.551 $\text{\AA}$	0.3 $\text{\AA}^a$
$K$	48.7 $\text{\AA}^{-16} \mu\text{sec}^{-1}$	
$\int g_s(E)g_a(E) dE$	0.71 $\text{eV}^{-1}$	
$N_{5s}N_{5p}$	$1.939 \times 10^{-4}$	
$s \int \Phi_{3d_i} r_{12}^{-1} \Phi_{3d_j} d\tau_1 d\tau_2$	0.44 $\text{eV}$	$\sim 1 \text{ eV}$

<sup>a</sup>From a fit to the free-atom antimony Hartree-Fock wave functions (Ref. 28) at  $R \gtrsim 1 \text{ \AA}$ .

When the exchange interaction of Eq. (14) is substituted into Eq. (5) with the parameters chosen as above, an excellent fit to the experimental donor decay curve is achieved. The fit is equally good for all concentrations and clearly shows the correct behavior as a function of concentration. Figure 5 shows the calculated and experimental curves for all the concentrations of manganese that were investigated. Each experimental curve is matched to the theoretical curve at  $t = 0.334 \mu\text{sec}$ , which is the starting time of the experimental scan. The theoretical curves are computed from  $t = 0$ .

Because the early nonexponential character of the antimony decay curve in the presence of quenching ions is a sensitive function of the range dependence of the interaction, the exchange parameters of Eq. (14) can be determined accurately. In Table II, we present these parameters and quantities derived from them. We also compare the results with quantities derived using atomic orbitals. Because of uncertainties in the measured spectral overlap integral and factors in the manganese defect  $3d$  wave function, only an order of magnitude comparison is made with  $\langle 3d_i | \tau_{12}^{-1} | 3d_j \rangle$ . The wave function of the defect is more delocalized than the atomic wave functions. However, we see that a rough calculation of the exchange interaction is in agreement with the yield and decay characteristics of the antimony luminescence, which strengthens our assignment of the energy transfer to exchange. We have also used the simpler exchange interaction suggested by Dexter<sup>20</sup> in place of Eq. (14).

$$P = Ke^{-2R/L}, \quad (19)$$

where  $L$  is an effective Bohr radius. Equation (19) has a sharper cutoff in its range than Eq. (14) and the fit to the decay curve goes below the experimental curve at early times and further above it at later times. On the other hand, a slightly more diffuse form of the exchange interaction than Eq. (14) which would better accommodate electron delocalization of the antimony wave function or superexchange interactions would undoubtedly fit the experimental curve to within the error of measurement. These



corrections are, however, minor.

We have assumed that energy transfer between antimony ions or diffusion is not important. Fast diffusion, which effectively averages out variations in transfer times for different donor-acceptor pairs and exhibits a simple exponential decay of the donor system with neither the decay time or yield depending on the acceptor concentration, can be ruled out. When the rate of energy diffusion within the donor system is slow but still comparable to the intrinsic relaxation time  $\tau$ , then diffusion to the vicinity of an acceptor competes with direct energy transfer. The decay curves will exhibit an early time nonexponential character corresponding to the direct energy transfer followed by an exponential decay with the approximate characteristic lifetime

$$\frac{1}{\tau_D} = \frac{1}{\tau} + 4\pi N_a D \rho,$$

where  $D$  is a diffusion constant and  $\rho$  is a length. We observed no dependence of the decay curves or yield on the antimony ion concentration in phos-

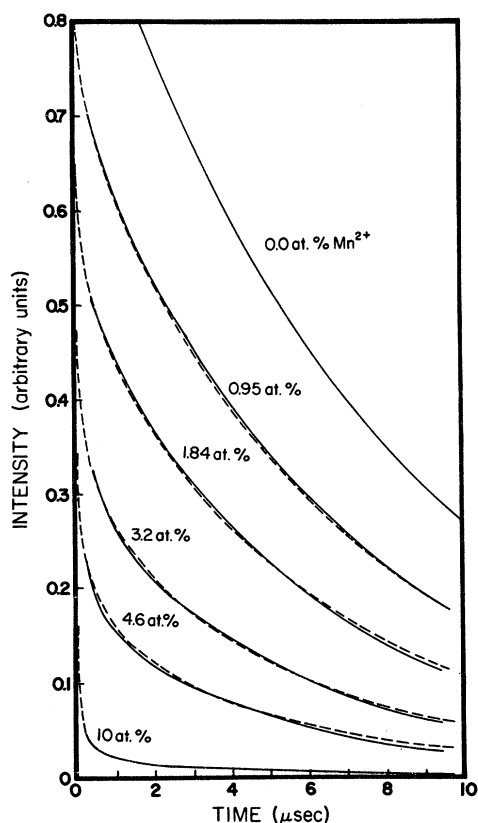


FIG. 5. The antimony luminescence decay curves as a function of manganese concentration and the theoretically calculated curves using the exchange interaction. The theoretical curves were normalized to unit intensity at time  $t=0$ . The experimental curves were scaled to the theoretical curves at the point  $t=0.334 \mu\text{sec}$ .

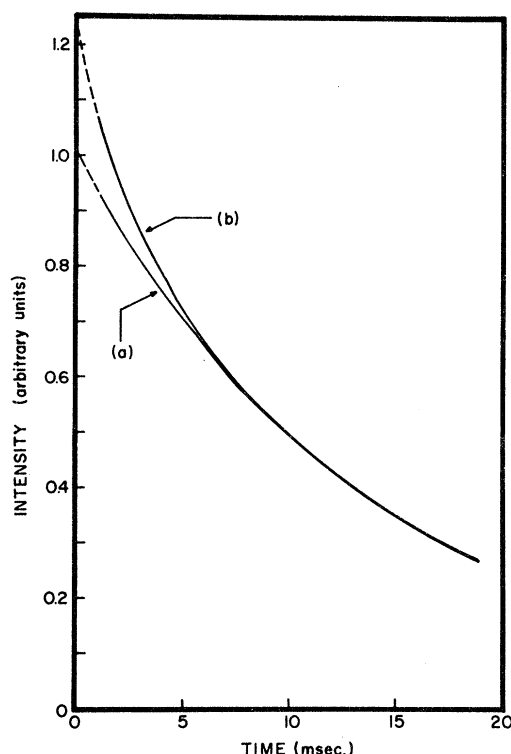


FIG. 6. The decay of manganese emission in fluorophosphate phosphors following excitation at 254 nm. Curve (a) was obtained from samples in which the antimony was charge compensated by  $\text{Na}^+$ . The dashed curve (a) is from  $e^{-t/14.3 \text{ msec}}$ . Curve (b) is the decay of manganese emission from samples in which antimony is charge compensated by oxygen. The dashed curve (b) is calculated from  $e^{-t/14.3} + 0.23 e^{-t/1.9}$ .

phors with analyzed antimony concentrations between 0.25 and  $\sim 1$  at. %. Botden<sup>33</sup> did observe evidence of antimony-antimony energy transfer at somewhat higher concentrations.

#### B. Manganese Emission

The manganese emission resulting from excitation by energy transfer from antimony in a normal codoped fluorophosphate exhibits a decay curve which departs from a simple exponential curve at early time ( $t < 6 \text{ msec}$ ). The decay curve can be fit quite well by the sum of two exponentials. When excitation is by energy transfer from antimony which is charge compensated by sodium, the short-lifetime component is absent, as shown in curve (a) of Fig. 6. This curve fits a single exponential with a lifetime  $\tau_1$  of  $14.3 \pm 0.5 \text{ msec}$ . When curve (a) is subtracted from curve (b) in Fig. 6, the remainder is exponential with a lifetime  $\tau_2$  of  $1.9 \pm 0.1 \text{ msec}$ . By integrating the areas under the exponential curves it is found that the short-lifetime component comprises only about 3% of the total manganese emission.

Confirmation that the complex manganese emission decay curve is due to the superposition of two exponential components, and not to energy transfer, is afforded by a wavelength dependence of the relative intensity of the two components. Using a monochromator to analyze the emission it was found that the relative intensity of the short-lifetime component is enhanced on the low-energy side of the manganese emission band and suppressed on the high-energy side. Therefore, although the short-lifetime component of the emission cannot be resolved from the primary manganese emission band, the peak of the short-lifetime component falls at a slightly lower energy.

In addition to the case where antimony is charge compensated by sodium, the short-lifetime component is also absent in samples activated with manganese only and in samples sensitized with  $\text{Sn}^{2+}$  which is isoelectronic with  $\text{Sb}^{3+}$ , but requires no charge compensation. These samples which have no short-lifetime component of the manganese emission all have the common feature of no oxygen-compensated antimony. Energy transfer from oxygen-compensated antimony will preferentially excite those manganese centers lying closest to antimony, while direct excitation of manganese by irradiation between 300 and 450 nm will not show this preference. The relative amount of short-lifetime manganese emission from a sample containing oxygen-compensated antimony is diminished when the manganese is excited directly, indicating that the manganese center responsible for the short-lifetime emission lies in physical proximity to the oxygen-compensated antimony. Such a center has been identified by Ryan and Vodoklys and labeled as  $\text{Mn}(\text{Sb})$ .<sup>12</sup> They found this center to comprise less than 5% of the total manganese centers by a comparison of the relative strengths of the excitation peaks. The proposed model for the  $\text{Mn}(\text{Sb})$

center is manganese at a  $\text{Ca}(\text{II})$  site adjacent to an antimony-oxygen complex.

## V. SUMMARY

The mechanism of energy transfer from antimony to manganese impurity ions in fluorophosphate phosphors has been investigated. Using order-of-magnitude arguments we showed that the energy transfer rate by dipole-dipole and dipole-quadrupole interactions was too small to account for the energy transfer. Further, in Sec. IV, we showed that both the donor yield and decay curve were characteristic of a short-range nonradiative exchange mechanism between antimony and manganese ions. From a careful measurement of the donor decay curve, we determined the rate constant and hence, information about the intermolecular exchange interaction. The energy transfer rate to the closest  $\text{Ca}(\text{I})$  site in the fluorophosphate lattice is  $10^{11} \text{ sec}^{-1}$  and energy transfer to manganese competes with radiative deexcitation of the donor ( $\tau = 7.65 \mu\text{sec}$ ) out to around  $12.9 \text{ \AA}$ . The manganese acceptor decay curve is dominated by a single exponential curve with a lifetime of 14.3 msec. We cannot eliminate the possibility that more than one manganese center behaves as an acceptor with similar intrinsic lifetimes.

## ACKNOWLEDGMENTS

We thank Dr. T. S. Davis for informing us of his earlier measurements of the lifetimes of antimony and manganese luminescence. We also thank B. Burts and Ed Yandek for technical assistance in making optical measurements and J. W. Hunter and M. Bradford for doing the chemical analysis. Finally the authors are very appreciative of valuable suggestions and comments by Dr. J. W. Richardson and Dr. F. E. Williams.

<sup>1</sup>E. Nakazawa and S. Shionoya, *J. Chem. Phys.* **47**, 3211 (1967); and Refs. 1–23. References 1–3 provide a representative sampling of published experimental studies of energy transfer in inorganic systems.

<sup>2</sup>L. G. Van Uitert, E. F. Dearborn, and J. J. Rubin, *J. Chem. Phys.* **47**, 3653 (1967); and Refs. 8–11.

<sup>3</sup>H. Nashimura, M. Tanaka, and M. Tomura, *J. Phys. Soc. Japan* **28**, 128 (1970); and Refs. 4–10.

<sup>4</sup>H. G. Jenkins, A. H. McKeag, and P. W. Randy, *J. Electrochem. Soc.* **96**, 1 (1949).

<sup>5</sup>For a good review of energy transfer in the triplet state see V. L. Ermoleav, *Usp. Fiz. Nauk* **80**, 3 (1963) [*Sov. Phys.-Usp.* **6**, 333 (1963)].

<sup>6</sup>A. N. Terenin and V. L. Ermoleav, *Dokl. Akad. Nauk SSSR* **85**, 547 (1952) (Engl. trans.: NRC TT-529).

<sup>7</sup>V. L. Ermoleav and A. N. Terenin, *Collection in Memory of S. I. Vavilov* (Viniti, Moscow, 1952), p. 137 (Engl. trans.: NRC TT-540).

<sup>8</sup>R. J. Birgeneau, *J. Chem. Phys.* **50**, 4282 (1969).

<sup>9</sup>R. J. Birgeneau, M. T. Hutchings, J. M. Baker, and J. D. Riley, *J. Appl. Phys.* **40**, 1070 (1969).

<sup>10</sup>M. Inokuti and F. Hirayama, *J. Chem. Phys.* **43**, 1978 (1965).

<sup>11</sup>P. H. Kasai, *J. Phys. Chem.* **66**, 674 (1962).

<sup>12</sup>F. M. Ryan and F. M. Vodoklys, *J. Electrochem. Soc.* **118**, 1814 (1971).

<sup>13</sup>T. Förster, *Ann. Physik* **2**, 55 (1948); *Z. Naturforsch.* **4a**, 321 (1949).

<sup>14</sup>M. Yokota and O. Tanimoto, *J. Phys. Soc. Japan* **22**, 779 (1967).

<sup>15</sup>M. J. Weber, *Phys. Rev. B* **4**, 2932 (1971).

<sup>16</sup>F. E. Williams, *Electrochem. Soc. Ext. Abst.* **9**, 40 (1960).

<sup>17</sup>F. M. Ryan, R. C. Ohlmann, J. Murphy, R. Mazelsky, G. R. Wagner, and R. W. Warren, *Phys. Rev. B* **2**, 2341 (1970).

<sup>18</sup>S. Naray-Szabo, *Z. Krist.* **75**, 387 (1930); as refined by A. S. Posner, A. Perloff, and A. F. Pioro, *Acta*

Cryst. **11**, 308 (1958).

<sup>19</sup>The decay of donor luminescence following steady-state excitation in the presence of dipole-dipole energy transfer is given by K. B. Eisenthal and S. Siegal, *J. Chem. Phys.* **41**, 652 (1964). See also footnote 37 in Ref. 10.

<sup>20</sup>D. L. Dexter, *J. Chem. Phys.* **21**, 836 (1953).

<sup>21</sup>T. F. Soules, T. S. Davis, and E. R. Kreidler, *J. Chem. Phys.* **55**, 1056 (1971).

<sup>22</sup>P. D. Johnson, in *Proceedings of Luminescence of Organic and Inorganic Materials* (Wiley, New York, 1962), p. 563.

<sup>23</sup>Koziro Norita, *J. Phys. Soc. Japan* **16**, 99 (1961).

<sup>24</sup>W. B. Fowler and D. L. Dexter, *Phys. Rev.* **128**, 2154 (1962).

<sup>25</sup>J. D. Axe and P. F. Weller, *J. Chem. Phys.* **40**,

3066 (1964).

<sup>26</sup>J. S. Griffith, *The Theory of Transition-Metal Ions* (Cambridge U. P., Cambridge, 1964), p. 112.

<sup>27</sup>A. M. Clogston, *J. Phys. Chem. Solids* **7**, 201 (1958).

<sup>28</sup>C. Froese, *Some Hartree-Fock Results for the Atoms Helium to Radon* (University of British Columbia, Vancouver, 1968).

<sup>29</sup>This value was obtained for the  $\text{Mn}^{2+}$  ion in  $\text{K}_4\text{Mn}(\text{CN})_6 \cdot 3\text{H}_2\text{O}$ . B. N. Figgis, *Trans. Faraday Soc.* **57**, 204 (1961).

<sup>30</sup>T. S. Davis, E. R. Kreidler, J. A. Parodi, and T. F. Soules, *J. Luminescence* **4**, 48 (1971).

<sup>31</sup>F. Perrin, *Compt. Rend.* **178**, 1978 (1924).

<sup>32</sup>V. L. Ermoleav, *Dokl. Akad. Nauk. SSSR* **139**, 348 (1961) [*Sov. Phys.-Doklady* **6**, 600 (1962)].

<sup>33</sup>Th. Botden, *Philips Research Rept.* **7**, 197 (1952).

PHYSICAL REVIEW B

VOLUME 7, NUMBER 4

15 FEBRUARY 1973

## Optical-Absorption Spectrum of Tetrahedral $\text{Fe}^{2+}$ in $\text{CdIn}_2\text{S}_4$ : Influence of a Weak Jahn-Teller Coupling

S. Wittekoek, R. P. van Staple, and A. W. J. Wijma

*Philips Research Laboratories, Eindhoven, Netherlands*

(Received 14 August 1972)

The optical absorption of  $\text{Fe}^{2+}$  ions substituted in the spinel  $\text{CdIn}_2\text{S}_4$  has been studied between 6 and 300 °K. For  $\text{Fe}^{2+}$  at tetrahedral sites, crystal field transitions have been observed at  $2500\text{ cm}^{-1}$  ( ${}^5E \rightarrow {}^5T_2$ ) and at  $13\,000\text{ cm}^{-1}$  ( ${}^5E \rightarrow {}^3T_1$ ). At liquid-helium temperature the  ${}^5E \rightarrow {}^5T_2$  transition shows a rich structure, attributed to the combined interaction of spin-orbit coupling and a Jahn-Teller active mode of vibration in the  ${}^5T_2$  state. The frequencies and intensities of the stronger absorption lines of this  ${}^5E \rightarrow {}^5T_2$  band are found to be in agreement with a numerical calculation of the energy-level scheme of the  ${}^5T_2$  state, assuming a spin-orbit coupling constant of  $70\text{ cm}^{-1}$  and the presence of a Jahn-Teller active mode of vibration of the iron-sulphur complex with a frequency of  $300\text{ cm}^{-1}$  and a Jahn-Teller coupling energy of  $210\text{ cm}^{-1}$ . The results are compared with calculations of the moments of the spectral distribution and with measurements of the phonon frequencies. The  ${}^5E$  ground state is split by second-order spin-orbit interaction. Measurements of the spectrum at different temperatures show that the two lowest sublevels of the  ${}^5E$  state are separated by  $18\text{ cm}^{-1}$ .

### I. INTRODUCTION

In magnetic compounds with spinel structure the presence of divalent iron on tetrahedral sites has a profound influence on the magnetic properties. In  $\text{FeCr}_2\text{S}_4$  and  $\text{Cd}_{1-x}\text{Fe}_x\text{Cr}_2\text{S}_4$  it has been found by magnetization,<sup>1</sup> Mössbauer,<sup>2</sup> and ferromagnetic-resonance experiments<sup>3</sup> that the anisotropy of these materials is associated with the  ${}^5E$  ground state of the  $\text{Fe}^{2+}$  ions which is split by the Cr-Fe exchange field and spin-orbit coupling. Direct information about the splitting of the lowest energy levels of the  $\text{Fe}^{2+}$  ions can be expected from optical-absorption measurements of the crystal field transitions of these ions. The lowest transition from the  ${}^5E$  ground state to the  ${}^5T_2$  excited state is expected to occur in the region between 2 and  $5\text{ }\mu\text{m}$ , where the sulphospinel is transparent. One expects this transition to show a complicated spec-

trum since apart from exchange and spin-orbit coupling the spectrum will also be influenced by lattice vibrations, especially by the Jahn-Teller active modes of the  ${}^5T_2$  state.

In this paper we will report optical absorption measurements of  $\text{Fe}^{2+}$  ions on tetrahedral sites in a sulphospinel, viz.  $\text{CdIn}_2\text{S}_4$ . In this diamagnetic compound a study of the  $\text{Fe}^{2+}$  spectrum is possible in the presence of spin-orbit and Jahn-Teller coupling but not complicated by the presence of an exchange field.

A knowledge of this spectrum should be a valuable aid when attacking the more complicated problem of the absorption of  $\text{Fe}^{2+}$  ions in magnetic compounds, e.g., in  $\text{CdCr}_2\text{S}_4:\text{Fe}^{2+}$  which we will undertake in the near future. Optical spectra of tetrahedral  $\text{Fe}^{2+}$  in other compounds, e.g., in  $\text{ZnS}$ ,  $\text{CdTe}$ , and  $\text{MgAl}_2\text{O}_4$ , have been reported earlier.<sup>4-6</sup> The most recent analysis of this type of spectra is